

Charge dynamics and possibility of ferromagnetism in $A_{1-x}La_xB_6$ ($A = Ca$ and Sr)K. Taniguchi,¹ T. Katsufuji,^{1,2,*} F. Sakai,³ H. Ueda,¹ K. Kitazawa,^{1,2} and H. Takagi¹¹ *Department of Advanced Materials Science, University of Tokyo, Tokyo 113-8656, Japan*² *Solution Oriented Research for Science and Technology (SORST), Japan Science and Technology Corporation, Kawaguchi 332-0012, Japan*³ *Institute for Solid State Physics, University of Tokyo, Kashiwa 277-8581, Japan*

(Received 15 March 2002; revised manuscript received 28 May 2002; published 2 August 2002)

Ferromagnetism was recently reported in La-doped alkaline-earth hexaborides $A_{1-x}La_xB_6$ ($A = Ca, Sr,$ and Ba). We have performed reflectivity, Hall resistivity, and magnetization measurements of $A_{1-x}La_xB_6$. The results indicate that $A_{1-x}La_xB_6$ can be regarded as a simple doped semimetal, with no signature of an excitonic state as suggested by several theories. It is also found that the surface of as-grown samples ($\sim 10 \mu\text{m}$ in thickness) has a different electronic structure from a bulk one, and a fairly large number of paramagnetic moments are confined in this region. After eliminating these paramagnetic moments at the surface, we could not find any evidence of an intrinsic ferromagnetic moment in our samples, implying the possibility that the ferromagnetism of $A_{1-x}La_xB_6$ reported so far is not intrinsic.

DOI: 10.1103/PhysRevB.66.064407

PACS number(s): 78.30.-j, 72.20.My, 75.50.Cc

I. INTRODUCTION

Recently, ferromagnetism with high T_C (~ 600 K) was reported in alkaline-earth hexaborides doped with La, $A_{1-x}La_xB_6$ ($A = Ca, Sr,$ and Ba).¹ According to the study, the magnitude of the ferromagnetic moment varies with La concentration x , and is at a maximum at $x=0.005$, though very tiny ($< 10^{-3} \mu_B/\text{unit cell}$). Since this series of compounds has no magnetic elements, the appearance of ferromagnetism is quite surprising and has stimulated a number of studies on the mechanism of ferromagnetism. The parent compound, alkaline-earth hexaboride, AB_6 , contains a CsCl arrangement of divalent alkaline-earth ions and B_6 clusters, and early theoretical work on the cluster calculation of B_6 indicated that a B_6 cluster with a transfer of two electrons (from the divalent alkaline-earth ion) takes a closed-shell electronic structure.² More detailed band calculations³⁻⁵ indicated that there is a band overlap at the X points of the Brillouin zone between the valence band formed by the B $2p$ state and the conduction band strongly hybridized with the alkaline earth d , and thus AB_6 is a semimetal. Many theoretical models⁶⁻⁸ for the ferromagnetism put their basis on an “excitonic” state of AB_6 , where the electrons and holes in a semimetal form triplet excitons as binding states. Extra electrons introduced by La substitution into such a state favors a parallel spin configuration to gain paring energy of excitons, and yields a ferromagnetic state as a result.

One of the important aspects of these theories is that the magnetic properties of $A_{1-x}La_xB_6$ are dominated by carrier doping. Such a doping-dependent ferromagnetism is analogous to the ferromagnetism of perovskite manganites, and experimental studies of charge dynamics are indispensable to clarify such ferromagnetism caused by carrier doping. However, there has been little systematic investigation of the electronic structure of $A_{1-x}La_xB_6$ as a function of La concentration. It should be stressed here that to know how electronic states evolve with La doping is the first step to experimentally understanding the possible relationship between

ferromagnetism and charge dynamics in $A_{1-x}La_xB_6$.

Another important issue from an experimental viewpoint is how to characterize samples properly. Recent studies of $A_{1-x}La_xB_6$ suggested a strong sample dependence as well as a spatial inhomogeneity of ferromagnetism.⁹⁻¹² Here, we have to be careful about the fact that the magnitude of the ferromagnetic moment is so small and can be easily affected by a small amount of impurities. It is very important, therefore, to characterize samples properly in terms of carrier concentration, possible spatial inhomogeneity, and impurity.

In the present study, we carry out an optical reflectivity measurement as well as a Hall measurement of $A_{1-x}La_xB_6$ with systematically changing x . These measurements are very powerful technique to obtain basic parameters for charge dynamics, for example, the effective mass and the concentration of carriers. Furthermore, the inhomogeneity of the sample can easily be checked by utilizing the microscopy technique of reflectivity measurement. The aim of the present study is to investigate the evolution of electronic structures as well as the variation of magnetic properties with La doping, and to clarify whether the charge dynamics is really related to the “ferromagnetism” of $A_{1-x}La_xB_6$.

II. EXPERIMENT

Single crystals of $A_{1-x}La_xB_6$ ($A = Ca$ and Sr , $0 \leq x \leq 0.02$) were grown by an Al flux method. $CaCO_3$ (4N), $SrCO_3$ (4N), LaB_6 (3N), boron (5N), and Al (4N) were used as starting materials and flux. CaB_6 or SrB_6 was made by borothermal reduction, and was put into an alumina crucible together with LaB_6 and Al. The materials were heated up to 1500°C and slowly cooled down under an Ar atmosphere.¹³ Plate-like samples with a (100) surface with a typical dimension of $1 \times 1 \times 0.1 \text{ mm}^3$ were obtained. The detail of the sample characterization is discussed in Sec. V. Hall measurement was performed by applying magnetic field between -5 and 5 T. The electrode was attached by directly melting and bonding Au wire onto the sample surface. Reflectivity was measured between 0.07 and 0.6 eV using a Fourier-transform

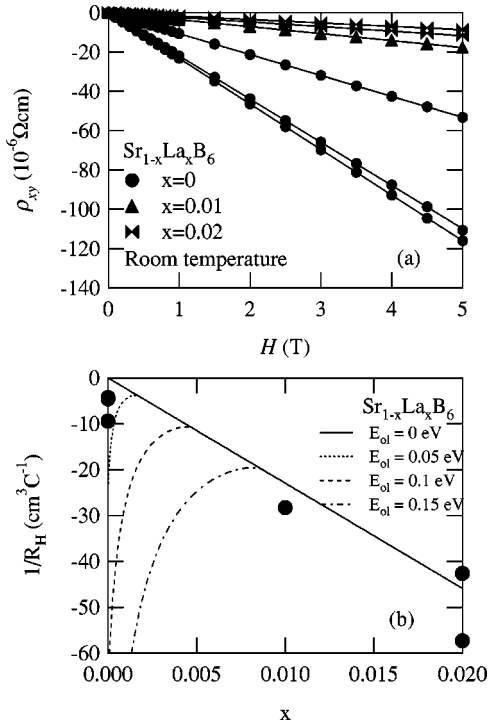


FIG. 1. (a) Hall resistivity vs magnetic field for $\text{Sr}_{1-x}\text{La}_x\text{B}_6$ at 300 K. The solid lines are least-square fits of the results to $\rho_{xy} = R_H H$. (b) Inverse Hall coefficients ($1/R_H$) as a function of La concentration x for $\text{Sr}_{1-x}\text{La}_x\text{B}_6$. The solid line shows the relation $1/R_H = xe$, and the dotted line, the dashed line, and the dot-dashed line show the calculated values of $1/R_H$ with the band overlap (E_{ol}) of 0.05, 0.1, and 0.15 eV, respectively.

infrared spectrometer equipped with a microscope. We checked the dependence of the spectra on the surface treatment, and the result is discussed in detail in Sec. IV. Magnetization was measured by a superconducting quantum interference device magnetometer. Since the volume of each single crystal was too small, more than ten pieces were combined for the magnetization measurement. In each measurement, a background signal was measured separately and subtracted from a total signal.

III. HALL MEASUREMENT

The Hall resistivity ρ_{xy} vs magnetic field H for $\text{Sr}_{1-x}\text{La}_x\text{B}_6$ at room temperature is shown in Fig. 1. In typical ferromagnetic metals, nonlinear behaviors of $\rho_{xy}(H)$ are often observed (the so-called anomalous Hall effect), particularly around T_C . This effect comes from an anomalous term of Hall resistivity proportional to magnetization, $R_s M$.¹⁴ However, $\rho_{xy}(H)$ of $\text{Sr}_{1-x}\text{La}_x\text{B}_6$ shows a linear dependence with no sign of the anomalous Hall effect for any composition, as shown in Fig. 1(a).

When the anomalous term does not exist, the Hall resistivity is given only by an ordinary term proportional to the magnetic field, $R_H H$. Figure 1(b) plots the inverse Hall coefficient $1/R_H$ as a function of x . The negative values of R_H mean that the majority carriers are electrons. The solid line gives the relation $1/R_H = -xe$. The agreement between the

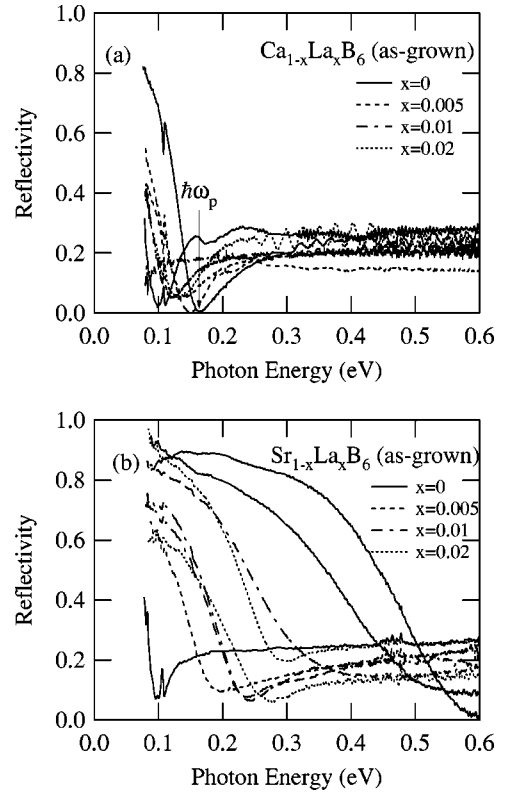


FIG. 2. Reflectivity spectra of (a) $\text{Ca}_{1-x}\text{La}_x\text{B}_6$ and (b) $\text{Sr}_{1-x}\text{La}_x\text{B}_6$ on an as-grown surface. The arrow shows the position of the plasma edge of a typical spectrum.

experimental results and the simple relation $1/R_H = -xe$ indicates that La doping introduces the same number of electrons into the conduction band. If the effect of band overlap in a semimetal is taken into account, the relation between the Hall coefficient and x becomes more complicated. This issue will be discussed in Sec. IV.

IV. REFLECTIVITY MEASUREMENT

Hall coefficients are dominated only by the number of carriers n , but do not reflect their effective mass m^* . On the other hand, a reflectivity spectrum can reveal the value of n/m^* through its plasma frequency $\omega_p = \sqrt{4\pi n e^2 / \epsilon_\infty m^*}$, where ϵ_∞ is the dielectric constant at higher than the plasma frequency.

Figure 2 shows the reflectivity spectra of $\text{Ca}_{1-x}\text{La}_x\text{B}_6$ and $\text{Sr}_{1-x}\text{La}_x\text{B}_6$ on as-grown surface as well as on a slightly polished surface (by $< 1 \mu\text{m}$ in depth). As can be seen, almost all the spectra have a clear plasma edge, as typically shown by an arrow, but the values of $\hbar\omega_p$ with the same composition are fairly scattered. In fact, it is found that even pieces from the same crucible show different $\hbar\omega_p$ values. As a result, a systematic variation of $\hbar\omega_p$ with x , which is expected from the Hall-coefficient measurement, is barely observed. As an overall feature, the Sr series have larger values of $\hbar\omega_p$ than the Ca series, similar to what was found in previous reports.^{11,15}

It should be noted here that reflectivity measurements detect only a sample surface with a penetration depth of light

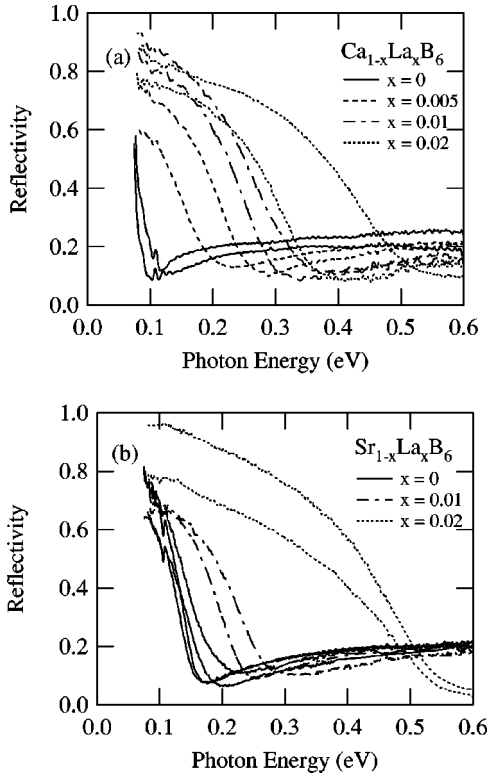


FIG. 3. Reflectivity spectra of (a) $\text{Ca}_{1-x}\text{La}_x\text{B}_6$ and (b) $\text{Sr}_{1-x}\text{La}_x\text{B}_6$ on the surface with filing ($\sim 10 \mu\text{m}$ in depth) and polishing.

(the order of μm). Thus if a sample surface of several μm in thickness has a different characteristic from the bulk one, the optical result can be inconsistent with the Hall measurement. To check for this possibility, we have filed the sample surface by $\sim 10 \mu\text{m}$ in depth, then polished it, and measured its reflectivity again. The reflectivity spectra after such surface treatment are shown in Fig. 3. The scattering of the $\hbar\omega_p$ values with the same composition is drastically suppressed, and it is clearly observed that $\hbar\omega_p$ shifts to higher energy with increasing x . We have also checked that there is almost no position dependence of the spectra along the sample surface.

To compare the experimental results with theoretical models, the ω_p value has been calculated based on the parameters from a band calculation.⁵ First, holes in the valence band are ignored and only electrons in the conduction band are taken into account. The band structure of AB_6 has electron pockets at the triply degenerate X point [(100), (010), and (001)], and the effective mass of the pocket is anisotropic between the longitudinal direction (parallel to the ΓX direction) and the transverse direction (perpendicular to the ΓX direction). According to a band calculation,⁵ the longitudinal mass (m_{el}) is $0.50m_0$ (m_0 is the free-electron mass) and the transverse mass (m_{et}) is $0.21m_0$. In this case, the plasma frequency ω_p is given by the equation

$$\omega_p = \sqrt{\frac{4\pi e^2}{\epsilon_\infty} \left(\frac{n_e/3}{m_{el}} + \frac{2n_e/3}{m_{et}} \right)}, \quad (1)$$

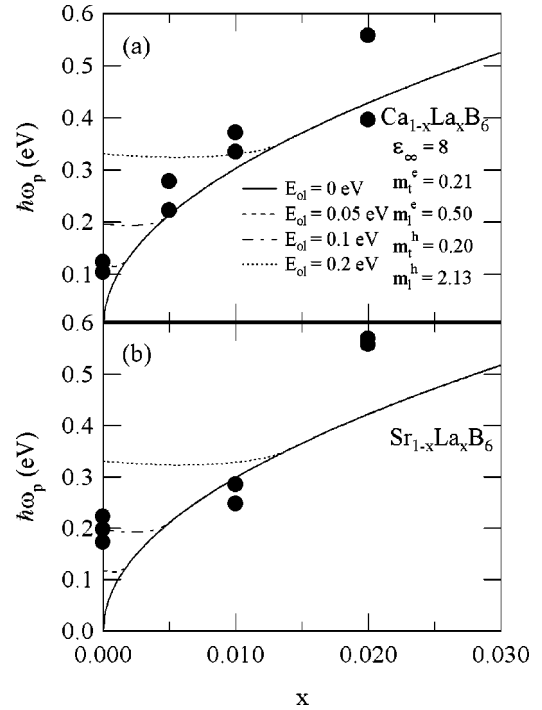


FIG. 4. Calculated values of $\hbar\omega_p$ for several values of band overlap E_{ol} (lines), and the experimental values of $\hbar\omega_p$ (closed circles) for (a) $\text{Ca}_{1-x}\text{La}_x\text{B}_6$ and (b) $\text{Sr}_{1-x}\text{La}_x\text{B}_6$.

where n_e is the number of electrons. ϵ_∞ is estimated to be 8 from a band calculation, which is consistent with the reflectivity value far above ω_p in the experiment (~ 0.22). The x dependence of $\hbar\omega_p$ calculated from Eq. (1) assuming $n_e = x$ (solid lines) as well as the experimental values of $\hbar\omega_p$ (closed circles) are plotted in Fig. 4. The agreement between the experiment and the calculation is quite satisfactory (except for $x=0$ as discussed later), indicating that the effective mass of the conduction band by the band calculation describes the charge dynamics of these compounds correctly.

One may note an evident discrepancy at $x=0$ between the experiment (finite values of $\hbar\omega_p$) and the calculation ($\hbar\omega_p = 0$). To calculate the $\hbar\omega_p$ value at $x \sim 0$, holes on the valence band, which exist even for $x=0$ in a semimetallic state, have to be taken into account. For the calculation, the effective mass of the valence band by the band calculation was used [the longitudinal mass (m_{hl}) is $2.13m_0$ and the transverse mass (m_{ht}) $0.20m_0$], but the band overlap (E_{ol}) was taken as a free parameter. In this case, the plasma frequency is given by the sum of the contribution from electrons and holes as

$$\omega_p = \sqrt{\frac{4\pi e^2}{\epsilon_\infty} \left(\frac{n_e/3}{m_{el}} + \frac{2n_e/3}{m_{et}} + \frac{n_h/3}{m_{hl}} + \frac{2n_h/3}{m_{ht}} \right)}, \quad (2)$$

where n_h is the number of holes, and $x = n_e - n_h$. The result of the calculation is shown in Fig. 4 for $E_{ol} = 0.05 \text{ eV}$ (the dotted line), 0.1 eV (the dashed line), and 0.2 eV (the dot-dashed line). From a comparison between the experiment and the calculation, the band overlap E_{ol} is estimated to be $\sim 0.05 \text{ eV}$ for CaB_6 , and $\sim 0.1 \text{ eV}$ for SrB_6 .

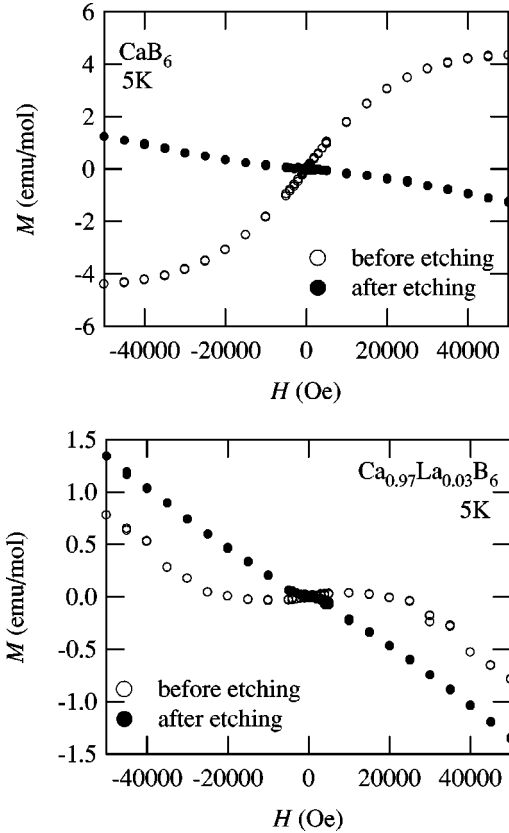


FIG. 5. Magnetization vs magnetic field at 5 K for CaB_6 (the upper panel) and $\text{Ca}_{0.97}\text{La}_{0.03}\text{B}_6$ (the lower panel) before (white circles) and after (closed circles) HNO_3 etching.

A similar calculation taking account of both electrons and holes can be made for Hall coefficients. In this case, the total Hall coefficient is given by the subtraction of the hole contribution from the electron contribution. The result is shown in Fig. 1(b), and, from the comparison in Hall coefficients, E_{01} is estimated to be <0.05 eV for SrB_6 . The discrepancy of the E_{01} values from reflectivity and Hall coefficients can be attributed to the deviation of the band structure from simple parabolic ones.

V. MAGNETIZATION MEASUREMENT

Since it has been clarified that the sample surface with $10 \mu\text{m}$ in thickness has a different electronic structure from the bulk one, the next question is how the magnetic properties of this part are different from the bulk magnetic properties. To answer this question, we first measured the magnetization of $A_{1-x}\text{La}_x\text{B}_6$, then etched the surface of the sample by HNO_3 , and measured its magnetization again. Figure 5 shows the magnetization of $\text{Ca}_{1-x}\text{La}_x\text{B}_6$ as a function of magnetic field before and after etching the sample. A drastic change of the magnetization before and after etching is clearly observed. Roughly speaking, a positive component (a ferromagnetic or a paramagnetic component) decreases, and a diamagnetic component survives with etching the sample surface. As most clearly seen in Fig. 6, the positive component is likely composed of both a ferromagnetic component,

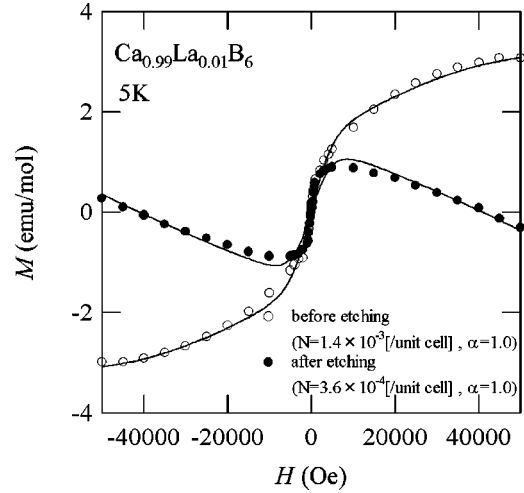


FIG. 6. Magnetization vs magnetic field for $\text{Ca}_{0.99}\text{La}_{0.01}\text{B}_6$ at 5 K before (white circles) and after (closed circles) HNO_3 etching. Solid lines are fitting results by Eq. (3) (see text).

which saturates far below 10 000 Oe, and a paramagnetic component, which gradually saturates up to 50 000 Oe. To know which component changes most with etching, the magnetization curve has been fitted by the sum of three components—a paramagnetic, ferromagnetic, and diamagnetic components—as

$$M = Ng\mu_B S B_S(X) + \alpha M_{\text{ferro}}(H) + \chi_{\text{dia}} H, \quad (3)$$

$$X = g\mu_B S H / k_B T,$$

where N is the number of paramagnetic moments, g the g factor of the spin, μ_B the Bohr magneton, $B_S(X)$ the Brillouin function, α the amount of ferromagnetic moments, $M_{\text{ferro}}(H)$ the magnetization curve for a ferromagnet, and χ_{dia} the diamagnetic susceptibility of core electrons. χ_{dia} was fixed to the value calculated from the diamagnetic susceptibility of Ca and six B ($\chi_{\text{dia}} = -5.9 \times 10^{-5} \text{ cm}^3/\text{mol}$). Figure 6 shows one of the fitting results. Here $S=1/2$ for $B_S(X)$ is adopted, which fits the data best. From this fitting, it is found that parameter α , representing the amount of ferromagnetic moments, does not change by etching, but N , the number of paramagnetic moments, decreases to $\sim 40\%$. Similar results were obtained for other samples. Therefore, it can be concluded that the ferromagnetic moments are distributed over the sample uniformly, whereas the paramagnetic moments are localized at the sample surface.

This result implies the importance of removing sample surface when one correctly estimates the bulk ferromagnetic moment of $A_{1-x}\text{La}_x\text{B}_6$. Therefore, we carefully removed the sample surface by HNO_3 etching, and measured the magnetization curve of $A_{1-x}\text{La}_x\text{B}_6$ with various values of x and estimated the ferromagnetic moment. The size of the ferromagnetic moment as a function of x in the present experiment is shown by closed circles in Fig. 7, where the data from Ref. 1 are also plotted by closed squares. As can be seen, the ferromagnetic moment in the present experiment is substantially smaller than that of Ref. 1, except for one sample ($x=0.01$), the same one shown in Fig. 6. These re-

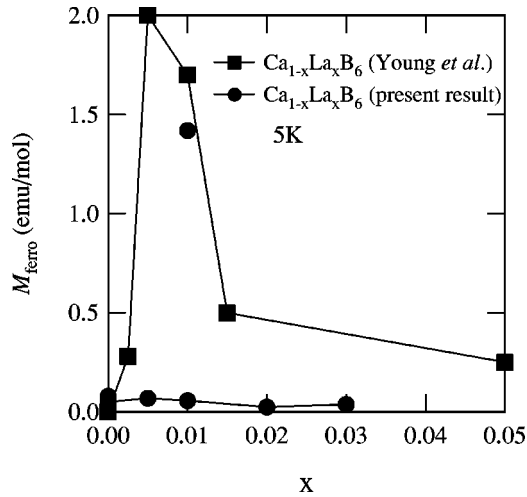


FIG. 7. Ferromagnetic moment vs La concentration x for $\text{Ca}_{1-x}\text{La}_x\text{B}_6$. Closed circles correspond to the present result, and closed squares to the result in Ref. 1.

sults suggest that the ferromagnetic moment is not intrinsic but is caused by some impurities in the sample.

To investigate what kind of and how much impurities exist in the sample, we took the following way. First, the magnetic impurities were searched qualitatively by x-ray fluorescence spectrometry. It was found from this technique that Fe is the main magnetic impurity in the sample. Then, we quantitatively determined the amount of Fe impurity by inductively coupled plasma atomic emission spectrometry (ICP-AES). Figure 8 shows the amount of Fe impurity (closed triangles), as well as the experimentally observed ferromagnetic moment of the same samples (closed circles). As can be seen, there is a rough correspondence between the amount of Fe impurity and the ferromagnetic moment. The $x=0.01$ sample with the largest ferromagnetic moment (as shown in Fig. 7) turned out to be the one containing the largest amount of Fe impurity (~ 1000 ppm, more than one order of magnitude larger than other samples). Furthermore, if we assume

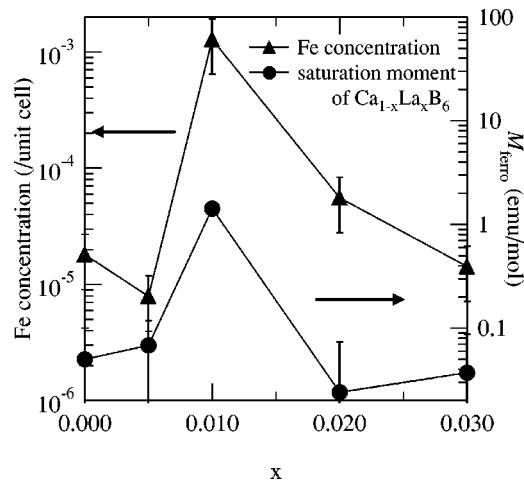


FIG. 8. Concentration of the Fe impurity (closed triangles, left axis) and ferromagnetic moment (closed circles, right axis) as a function of x for $\text{Ca}_{1-x}\text{La}_x\text{B}_6$.

$1 \mu_B$ moment per Fe, 7.3 emu/mol is expected in total, which exceeds the experimentally observed ferromagnetic moment, 1.4 emu/mol. On the other hand, other samples showing much smaller sizes of ferromagnetic moment (less than 0.1 emu/mol) have much smaller amounts of Fe impurity (less than 50 ppm), but they are also enough to produce the observed ferromagnetic moment. Therefore, we conclude that the ferromagnetic moment observed in the present experiment is caused by an Fe impurity.¹⁶

VI. DISCUSSION

One of the conclusions from the reflectivity measurement is that $A_{1-x}\text{La}_x\text{B}_6$ can be regarded as a simple doped semimetal, and no signature of an “excitonic state” has been observed in our reflectivity spectra for any x . Though we cannot completely exclude the possibility that such a feature exists outside of our experimental range (<0.07 eV), further evidence against the excitonic state in doped samples can be derived in the following way: The calculated lines for the finite values of E_{ol} in Fig. 4 merge into the solid line (for $E_{ol}=0$) at large x , where the Fermi level is located higher than the top of the valence band and the holes in the valence band are filled up. As can be seen in Fig. 4, the ω_p values in the experiment for $x \geq 0.005$ are in such a region, indicating that 0.5% La doping is enough to fill up the holes in the valence band. This indicates that the excitonic state, even if it exists for $x=0$, has already disappeared for $x=0.005$.

Recent band calculation by the so-called GW approximation indicated that stoichiometric CaB_6 is not a semimetal but a narrow-gap band insulator,¹⁷ and an angle-resolved photoemission experiment indicated the existence of a band gap and a Fermi level located at the conduction band, resulting in only electron pockets.¹⁸ These results are inconsistent with the interpretation of our experimental results based on a semimetal model. For this issue, we cannot exclude the possibility that the plasma edge for $x=0$ comes from doped electrons into the conduction band of a band insulator. In other words, it is possible that the size of the band overlap is zero (solid lines in Fig. 4), but the x axis in Fig. 4 is shifted by ~ 0.002 for Ca series and by ~ 0.005 for Sr series because of off-stoichiometry (most probably a B defect). However, it should be pointed out that we measured a number of pieces of the same composition, and found that $\hbar\omega_p$ is ~ 0.1 eV for all CaB_6 samples and ~ 0.2 eV for all SrB_6 samples. This can be easily explained by a semimetal model, as discussed in Sec. IV. From the doped insulator model, on the other hand, we have to assume that the amount of defects barely depends on samples, which seems fairly unlikely.

It is also found from the reflectivity measurement that the sample surface of $\sim 10 \mu\text{m}$ in thickness has a different electronic structure from the bulk one. This phenomenon seems generic for single crystals of these compounds grown under Al flux, judging from the results of previous optical studies by other groups.^{11,15} Since the phonon peak in the optical spectra around 0.11 eV, which is assigned to an internal mode of the B_6 cluster,¹⁹ is the same in energy before and after surface treatment, the surface state should be close to the bulk $A_{1-x}\text{La}_x\text{B}_6$ in terms of crystal structure. Possible

origins of the surface state could be a slightly oxidized phase or an off-stoichiometric phase precipitated at low temperatures during single-crystal growth. Whichever is the case, such an effect changes the Fermi level, or even changes the band structure, and thus varies the plasma frequency.

Let us move on to the magnetism of $A_{1-x}La_xB_6$. As discussed in Sec. V, both a ferromagnetic and a paramagnetic component coexist in the magnetization. The existence of a paramagnetic component in addition to a ferromagnetic component has not been explicitly discussed so far, but was already observed in various experiments (for example, high-field magnetizations in Ref. 20). It is found from the present experiment that paramagnetic moments are confined to the sample surface. What is the origin of these paramagnetic moments at the surface? The amount of the Fe impurity at the surface is estimated from ICP-AES, but the value is not large enough to explain the experimentally obtained size of the paramagnetic moment. It is reasonable to think that the electronic structure of the surface, which is different from the bulk one as shown in the reflectivity spectrum, is related to the appearance of the paramagnetic moment. One possibility is that the defect of Ca or B at the sample surface yields a local magnetic moment, as suggested by a recent calculation.²¹ However, further studies are necessary to understand the origin of the paramagnetic moment at the sample surface.

Regarding the ferromagnetism of $A_{1-x}La_xB_6$, the conclusion of the present experiment is that there is no intrinsic bulk ferromagnetic moment in our samples, but there is ferromagnetic moments caused by an Fe impurity. It should be stressed here again that our sample is well characterized in terms of carrier concentration, and it is unlikely that we missed the concentration range for an intrinsic ferromagnetic phase, if there is such a phase. Therefore, our best statement concerning this issue is that the ferromagnetism of

$A_{1-x}La_xB_6$ is not dominated by carrier doping. A plausible explanation is that any “ferromagnetism” of $A_{1-x}La_xB_6$ reported so far is caused by an Fe impurity, as is the case for our samples.

VII. SUMMARY

We have investigated the charge dynamics of $A_{1-x}La_xB_6$ by reflectivity and Hall measurement. It is found that La doping introduces the same number of electrons into a semi-metallic state, and its effective mass is consistent with a band calculation. No evidence of an excitonic state is observed, but the system should be regarded as a simple doped semimetal. It is also found that the as-grown sample surface with $\sim 10 \mu\text{m}$ in thickness has a different electronic structure from a bulk one. From magnetization measurements, it is found that this surface part contains a large number of paramagnetic moments. We have carefully measured the ferromagnetic moment of $A_{1-x}La_xB_6$ after removing the surface part by an etching process, and found that the ferromagnetic moments in our samples are substantially smaller than those observed so far. This result, together with a good correspondence between the size of the ferromagnetic moment and the amount of the Fe impurity in the sample, indicates that the “ferromagnetism” of $A_{1-x}La_xB_6$ is not intrinsic, but most probably caused by an Fe impurity.

ACKNOWLEDGMENTS

We thank M. Nohara, Z. Hiroi, and S. Horii for their help with sample growth at the early stage of this study, and Z. Fisk, S. Fujiyama, and M. Takigawa for helpful discussions. The present work was partly supported by a Grant-In-Aid for Scientific Research from the Ministry of Education, Culture, Sports, Science and Technology, Japan.

*Present address: Department of Physics, Waseda University, Tokyo 169-8555, Japan.

¹D.P. Young, D. Hall, E. Torelli, Z. Fisk, J.L. Sarrao, J.D. Thompson, H.R. Ott, S.B. Oseroff, R.G. Goodrich, and R. Zysler, *Nature* (London) **397**, 412 (1999).

²H.C.L. Higgins and M. de V. Roberts, *Proc. R. Soc. London, Ser. A* **224**, 336 (1954).

³A. Hasegawa and A. Yanase, *J. Phys. C* **12**, 5431 (1979).

⁴S. Massidda, A. Continenza, T.M. de Pascale, and R. Monnier, *Z. Phys. B: Condens. Matter* **102**, 83 (1997).

⁵C.O. Rodriguez, R. Weht, and W.E. Pickett, *Phys. Rev. Lett.* **84**, 3903 (2000).

⁶M.E. Zhitomirsky, T.M. Rice, and V.I. Anisimov, *Nature* (London) **402**, 251 (1999).

⁷L. Balents and C.M. Varma, *Phys. Rev. Lett.* **84**, 1264 (2000).

⁸V. Barzykin and L.P. Gor'kov, *Phys. Rev. Lett.* **84**, 2207 (2000).

⁹S. Kunii, *J. Phys. Soc. Jpn.* **68**, 3189 (1999).

¹⁰T. Terashima, C. Terakura, Y. Umeda, N. Kimura, H. Aoki, and S. Kunii, *J. Phys. Soc. Jpn.* **69**, 2423 (2000).

¹¹P. Vonlanthen, E. Felder, L. Degiorgi, H.R. Ott, D.P. Young, A.D. Bianchi, and Z. Fisk, *Phys. Rev. B* **62**, 10 076 (2000).

¹²R.R. Urbano, C. Rettori, G.E. Barberis, M. Torelli, A. Bianchi, Z.

Fisk, P.G. Pagliuso, A. Malinowski, M.F. Hundley, J.L. Sarrao, and S.B. Oseroff, *Phys. Rev. B* **65**, 180407(R) (2002).

¹³Another possible way of growing single crystals is to synthesize $Ca_{1-x}La_xB_6$ powder by borothermal reduction and to put it in Al flux. We believe that the difference should not affect the physical properties of the sample, as long as the carrier concentration is characterized correctly.

¹⁴See, for example, J.J. Rhyne, *Phys. Rev.* **172**, 523 (1968), and references therein.

¹⁵H.R. Ott, M. Chernikov, E. Felder, L. Degiorgi, E.G. Moshopoulou, J.L. Sarro, and Z. Fisk, *Z. Phys. B: Condens. Matter* **102**, 337 (1997)

¹⁶To investigate where these Fe impurities come from, we also determined the amounts of Fe impurity of the starting materials by ICP-AES. The amounts of Fe impurity are 6 ppm for $CaCO_3$, 2 ppm for B, 1040 ppm for LaB_6 , and 2 ppm for Al. On the basis of these values, we can explain Fe impurity less than 50 ppm in the single crystals by assuming that the Fe impurity of starting materials was slightly condensed to the crystals in the process of flux growth. However, for the one with the largest ferromagnetic moment (1 emu/mol), which has 1000-ppm Fe impurity, we guess that it is owing to an accidental contamination during synthesis.

- ¹⁷H.J. Tromp, P. van Gelderen, P.J. Kelly, G. Brocks, and P.A. Bobbert, Phys. Rev. Lett. **87**, 016401 (2001).
- ¹⁸J.D. Denlinger, J.A. Clack, J.W. Allen, G.-H. Gweon, D.M. Poirier, C.G. Olson, J.L. Sarrao, A.D. Bianchi, and Z. Fisk, cond-mat/0107429 (unpublished).
- ¹⁹L. Degiorgi, E. Felder, H.R. Ott, J.L. Sarrao, and Z. Fisk, Phys. Rev. Lett. **79**, 5134 (1997).
- ²⁰D. Hall, D.P. Young, Z. Fisk, T.P. Murphy, E.C. Palm, A. Teklu, and R.G. Goodrich, Phys. Rev. B **64**, 233105 (2001).
- ²¹R. Monnier and B. Delley, Phys. Rev. Lett. **87**, 157204 (2001).